



**Table 1.** In Vitro Inhibition of CCL2 Induced Chemotaxis of THP-1 Leukocytes<sup>a</sup>

lactam	ED <sub>50</sub> (nM)	lactam	ED <sub>50</sub> (nM)
( <i>S</i> )- <b>4</b>	15	( <i>S</i> )- <b>14</b>	7
( <i>S</i> )- <b>5</b>	0.09	( <i>S</i> )- <b>15</b>	0.09
( <i>R</i> )- <b>5</b>	4.5	( <i>R</i> )- <b>15</b>	0.44
( <i>S</i> )- <b>6</b>	0.08	( <i>S</i> )- <b>16</b>	0.8
( <i>S</i> )- <b>7</b>	0.2	( <i>S</i> )- <b>17</b>	0.09
( <i>S</i> )- <b>8</b>	0.5	( <i>S</i> )- <b>18</b>	0.5
( <i>S</i> )- <b>9</b>	1	( <i>S</i> )- <b>19</b>	0.8
( <i>S</i> )- <b>10</b> <sup>b</sup>	3	( <i>S</i> )- <b>20</b>	0.07
( <i>S</i> )- <b>11</b>	5	( <i>S</i> )- <b>21</b>	0.04
( <i>S</i> )- <b>12</b>	10	( <i>S</i> )- <b>22</b>	9
( <i>S</i> )- <b>13</b>	4	( <i>S,S</i> )- <b>23</b>	200

<sup>a</sup> Human myelomonocytic THP-1 cells. <sup>b</sup> A 50:50 mixture of diastereoisomers at the 2'-stereocenter.

**Table 2.** In Vitro Inhibition of Chemotaxis by (*S*)-**5**<sup>a</sup>

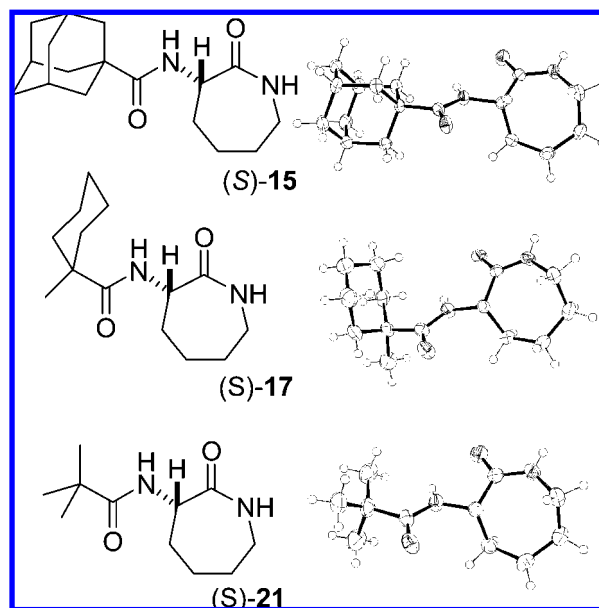
chemoattractant	cell type <sup>a</sup>	ED <sub>50</sub> (nM)
CCL2	THP-1	0.09
CCL3	THP-1	0.15
CCL5	THP-1	0.9
CXCL8	PMNC	0.3
CXCL12	THP-1	1
C5a	PMNC	>1000

<sup>a</sup> Human myelomonocytic THP-1 cells, or human peripheral blood polymorphonuclear cells (PMNC).

similar potency, making this compound a true broad spectrum chemokine inhibitor (BSCI). Notably, lactam (*S*)-**5** does not inhibit chemotaxis induced by the nonchemokine chemoattractant C5a. Lactam (*S*)-**5** itself does not possess any chemoattractant activity nor exhibits any cell toxicity or any effect on cell size, which can result in misinterpretation of data from the chemotaxis assay (see Supporting Information).<sup>10</sup>

The lactams inhibit migration in response to a range of chemokines with broadly similar potencies (within a factor of 10-fold), and changes in the lactam structure have similar effects on the potency against all the chemokines tested. This profile indicates that these compounds are not chemokine receptors antagonists acting at multiple receptors but that the BSCI compounds bind to cells at a single site and inhibit chemokine-induced migration by a yet-to-be understood mechanism. Consistent with this view, related BSCIs have been shown to neither bind to nor down-regulate any of a range of chemokine receptors nor to interfere with chemokine ligand or receptor dimerization.<sup>8a</sup> BSCIs cannot, therefore, be considered to be traditional chemokine antagonists.

Other 2',2'-dimethylated compounds (**6**–**9**) are also very potent in the CCL2/THP-1 chemotaxis assay, but monosubstituted side-chains (**10**–**12**) are less active. Unsaturation in the chain reduces potency (**6** vs **7**, **8** vs **9**, **10** vs **12**). The 3,3-dimethylated compound, (*S*)-**13**, is 40 times less potent than its isomer (*S*)-**5**. While bicyclooctane derivative (*S*)-**14** is a relatively poor inhibitor, adamantanes such as **15** are as potent as noncyclic lactams **5** and **6**, and once again the (*R*)-enantiomer is markedly less active. The non-2',2'-disubstituted analogue **16** is again less active, but significant loss of most of the adamantane structure (**17**–**21**) leads to little loss of activity as long as the quaternary 2-carbon of the side-chain is left intact. Indeed, lactams (*S*)-**20** and (*S*)-**21** are more potent than their larger analogues (70 and 40 pM, respectively). Chlorination (**22**) and dimerization (**23**) reduces potency. These studies demonstrate that the presence of a quaternary carbon at the 2-position of the side chain dramatically increases the potency of aminolactam BSCIs. X-ray crystal structures of compounds (*S*)-**15**, (*S*)-**17**, and

**Figure 2.** X-ray crystal structures of compounds (*S*)-**15**, (*S*)-**17**, and (*S*)-**21** (one of three in the unit cell). Ellipsoids are shown at 50% probability.

(*S*)-**21** are shown in Figure 2. In the crystal of compound (*S*)-**17**, the methyl group is in the equatorial position while the amide substituent is in the axial position. The energy difference between this conformation and one with an axial methyl and equatorial amide is probably small, and either conformation may be the active one. The side chain of the “axial–methyl” conformation of (*S*)-**17** can however be overlaid with the majority of the carbons of the adamantane in compound (*S*)-**15** (Scheme 1).

Representative potent compounds (*S*)-**5**, (*S*)-**15**, (*S*)-**17**, and (*S*)-**21** were then tested for anti-inflammatory potency in vivo. As previously, we adopted the murine sublethal lipopolysaccharide (LPS<sup>a</sup>) induced endotoxemia as a rapid in vivo screen of anti-inflammatory activity, using serum tumour necrosis factor- $\alpha$  (TNF- $\alpha$ ) measured 2 h after an intraperitoneal LPS injection as the end point. The lactams when administered via either the subcutaneous or oral routes inhibited LPS-stimulated TNF- $\alpha$  production with an ED<sub>50</sub> of as little as 0.1  $\mu$ g/kg and maximal effect of ~90%. (Table 3, Figure 3, (*S*)-**21**) This extraordinary anti-inflammatory potency is 1000 times greater than the previous unbranched lactams<sup>7</sup> and roughly 30 times more potent than the widely used “gold-standard” anti-inflammatory steroid dexamethasone (see Supporting Information for details). Interestingly, shortening of the long lipophilic side-chain (**5**–**21**) increases oral potency by over 1000 times.

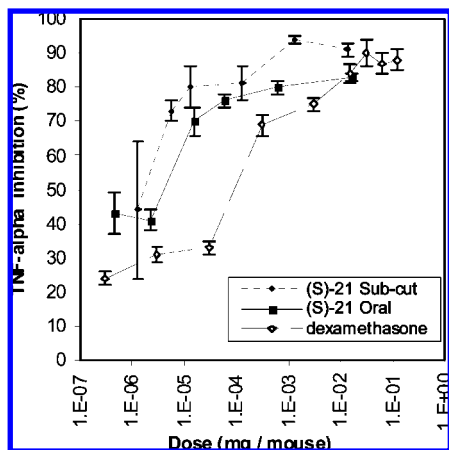
The pharmacokinetics of compounds (*S*)-**5**, (*S*)-**15**, (*S*)-**17**, and (*S*)-**21** following single dose administration in rat were also determined (Table 4). Consistent with the observations in the endotoxemia model, the shortened side chain of (*S*)-**21** compared with (*S*)-**5** resulted in a marked increase in exposure by both intravenous and oral administration as well as a substantial increase in fractional bioavailability by the oral route. The volume of distribution was also lower (close to total body water), suggesting that unwanted tissue accumulation resulting from the lipophilicity of long-chain-containing lactam (*S*)-**5** was essentially absent with trimethylacetylated lactam (*S*)-**21**.

<sup>a</sup> Abbreviations: LPS, lipopolysaccharide; TNF- $\alpha$ , tumour necrosis factor - $\alpha$ .

**Table 3.** In Vivo Anti-inflammatory Activity Measured by Inhibition of LPS Induced TNF- $\alpha$ 

lactam	ED <sub>50</sub> <sup>a</sup> $\mu$ g/kg (subcut)	maximum inhibitory effect % <sup>b</sup>	ED <sub>50</sub> <sup>a</sup> $\mu$ g/kg (oral)	maximum inhibitory effect % <sup>b</sup>
(S)-5	0.15	70	300	70
(S)-15	2	90	0.5	90
(S)-17	0.33	90	0.33	90
(S)-21	0.1	90	0.1	80
dex <sup>c</sup>	3	90	d	d

<sup>a</sup> See Supporting Information for full data. <sup>b</sup> % relative to control. <sup>c</sup> Dexamethasone. <sup>d</sup> Oral assay for dexamethasone was not performed.

**Figure 3.** Inhibition of LPS induced TNF- $\alpha$  in vivo by (S)-21 (subcutaneous and oral dose) and dexamethasone (subcutaneous dose).**Table 4.** Pharmacokinetic Parameters Following a Single Dose in Rat

	(S)-5	(S)-15	(S)-17	(S)-21
Intravenous Route (1 mg/kg)				
half-life (mins)	46	16	11	121
clearance (mL/min/kg)	40	84	55	6.8
V <sub>ss</sub> (L/kg) <sup>a</sup>	2.0	0.8	0.6	0.7
exposure (min·ng/mL)	23700	477	2900	231500
Oral Route (3 mg/kg)				
F (%) <sup>b</sup>	16	<1	5	71
half-life (min)	102	nd <sup>d</sup>	nd <sup>d</sup>	168
C <sub>max</sub> (ng/mL)	60	nd <sup>d</sup>	3	989
exposure (min·ng/mL) <sup>c</sup>	11000	nd <sup>d</sup>	430	493000

<sup>a</sup> Volume of distribution at steady state. <sup>b</sup> F = fractional bioavailability by the oral route. <sup>c</sup> Exposure = AUC(0→t). <sup>d</sup> n.d. = not determined, because the drug concentration in plasma was below the lower limit of quantitation of the assay (approximately 2 ng/mL) at all time points.

In contrast, although lactams (S)-15 and (S)-17 were also highly active in the endotoxemia model, both compounds achieve very poor exposure (Table 4). This apparent paradox is explained by investigation of the metabolic fate of the compounds. Adamantane (S)-15 is rapidly converted to the 3'-hydroxy derivative, presumably by a cytochrome P450 enzyme, on first pass through the liver, and this hydroxy-adamantane analogue is as active as the parent compound both in vitro and in vivo (data not shown). Similarly, cyclohexane (S)-17 is also rapidly hydroxylated, although the structures (and biological activities) of its primary metabolites are not known. Of the compounds studied here, therefore, it is trimethylacetyl-amino-lactam (S)-21 that has the most promising combination of DMPK properties and anti-inflammatory potency for further development as a pharmaceutical agent.

Despite being small and simple, the molecules described here will likely display complex pharmacology. For the most part, this reflects the complexity of the immune system. For example, in vivo the compounds do not achieve 100%

inhibition of LPS induced increases in TNF- $\alpha$ , even at concentrations when the molecular target is likely to be saturated. Indeed this substantial, but incomplete, inhibition may contribute to the promising profile of these lactam BSCIs as anti-inflammatory agents against a broad range of disease models. However, this same complexity also hampers a full understanding of the mode of action in vivo, and further investigations are clearly warranted.

## Conclusion

The inclusion of branching at the  $\alpha$ -carbon of the side chains of 3-acylamino-caprolactams greatly increases their in vitro and in vivo potency as broad-spectrum chemokine inhibitors. In addition, these features have also increased the activity of these compounds by oral administration significantly. Overall, the ease of chemical synthesis combined with the outstanding potencies of these molecules should lead to the first BSCI entering clinical trials as powerful anti-inflammatory drugs, potentially useful for the treatment of a wide range of conditions.

## Experimental Section

**Synthesis of Selected Compounds.** Full synthetic details and characterization data, including elemental analyses, are given in the Supporting Information. All compounds tested are >95% pure by elemental analysis. Proton NMR spectra were recorded on a Bruker Avance 500 Fourier transform spectrometer using an internal deuterium lock. Chemical shifts are quoted in parts per million downfield of tetramethylsilane, and values of coupling constants (*J*) are given in Hz.

**(S)-3-(2',2'-Dimethyl-dodecanoyl)amino-caprolactam (S)-5.** (S,S)-3-Amino-caprolactam hydro-pyrrolidine-5-carboxylate (2 mmol) and Na<sub>2</sub>CO<sub>3</sub> (6 mmol) in water (25 mL) were added to a solution of 2,2-dimethyl-dodecanoyl chloride (2 mmol) in dichloromethane (25 mL) at ambient temperature and the reaction mixture was stirred for 2 h. The organic layer was then separated, and the aqueous phase was extracted with additional dichloromethane (2 × 25 mL). The combined organic layers were dried over Na<sub>2</sub>CO<sub>3</sub> and reduced in vacuo. The residue was purified by silica column chromatography (eluent:EtOAc to 9:1 EtOAc:MeOH) to give (S)-3-(2',2'-dimethyl-dodecanoyl)amino-caprolactam (543 mg; 80%);  $\delta_{\text{H}}$  (500 MHz, CDCl<sub>3</sub>) 7.08 (1H, d, *J* 5.5, CHNH), 6.67 (1H, br s, CH<sub>2</sub>NH), 4.44 (1H, dd, *J* 11, 5.5, CHNH), 3.28–3.15 (2H, m, CH<sub>2</sub>NH), 2.01 (1H, br d, *J* 13, ring CH), 1.98–1.89 (1H, m, ring CH), 1.84–1.72 (2H, m, ring CH), 1.47–1.30 (3H, br m, ring CH + CH<sub>2</sub>CMe<sub>2</sub>CONH), 1.27–1.15 (17H, br m, ring CH + (CH<sub>2</sub>)<sub>8</sub>) 1.13 (3H, s, CMeMe), 1.12 (3H, s, CMeMe), and 0.82 (3H, t, *J* 7, CH<sub>2</sub>CH<sub>3</sub>).

**(S)-3-(1'-Adamantanecarbonyl)amino-caprolactam (S)-15.** (S)-3-amino-caprolactam hydrochloride (1 mmol) and Na<sub>2</sub>CO<sub>3</sub> (3 mmol) in water (15 mL) were added to a solution of 1-adamantanecarbonyl chloride (1 mmol) in dichloromethane (15 mL) at ambient temperature and the reaction was stirred for 2 h. The organic layer was then separated, and the aqueous phase was extracted with additional dichloromethane (2 × 25 mL). The combined organic layers were dried over Na<sub>2</sub>CO<sub>3</sub> and reduced in vacuo. The residue was recrystallized from CH<sub>2</sub>Cl<sub>2</sub>/hexanes to give (S)-3-(1'-adamantanecarbonyl)amino-caprolactam (171 mg, 59%);  $\delta_{\text{H}}$  (500 MHz, CDCl<sub>3</sub>) 7.08 (1H, d, *J* 5.5, CHNH),

6.67 (1H, br s, CH<sub>2</sub>NH), 4.47 (1H, ddd, *J* 11, 5.5, 1.5, CHNH), 3.32–3.17 (2H, m, CH<sub>2</sub>NH), 2.06–1.94 (5H, m, 2 × ring CH + 3 × adamantane CH), 1.90–1.75 (8H, m, 2 × ring CH + 3 × adamantane CH<sub>2</sub>), 1.72 (3H, br d, *J* 14.5, 3 × adamantane CHH), 1.68 (3H, br d, *J* 14.5, 3 × adamantane CHH), and 1.47–1.32 (2H, m, 2 × ring CH).

**(S)-3-(1'-Methylcyclohexanecarbonyl)amino-caprolactam (S)-17.** (S,S)-3-amino-caprolactam hydro-pyrrolidine-5-carboxylate (5 mmol) and Na<sub>2</sub>CO<sub>3</sub> (15 mmol) in water (25 mL) were added to a solution of 1-methylcyclohexanecarbonyl chloride (5 mmol) in dichloromethane (25 mL) at ambient temperature and the reaction was stirred for 12 h. The organic layer was then separated, and the aqueous phase was extracted with additional dichloromethane (2 × 25 mL). The combined organic layers were dried over Na<sub>2</sub>CO<sub>3</sub> and reduced in vacuo. The residue was purified by recrystallization from EtOAc/hexane to give the lactam (540 mg, 43%); δ<sub>H</sub> (500 MHz, CDCl<sub>3</sub>) 7.12 (1H, d, *J* 5, CHNH), 6.52 (1H, br s, CH<sub>2</sub>NH), 4.48 (1H, ddd, *J* 11, 5.5, 1.5 CHNH), 3.30–3.16 (2H, m, CH<sub>2</sub>NH), 2.01 (1H, br d, *J* 13, lactam ring CH), 1.98–1.86 (3H, m, lactam ring CH + cyhex CH × 2), 1.85–1.73 (2H, m, lactam ring CH × 2), 1.56–1.47 (2H, m, cyhex CH × 2), 1.47–1.33 (5H, br m, lactam ring CH × 2 + cyhex CH × 3) and 1.33–1.25 (3H, m, cyhex CH × 3).

**(S)-3-(2',2'-Dimethyl-propionyl)amino-caprolactam (S)-21.** (S,S)-3-amino-caprolactam hydro-pyrrolidine-5-carboxylate (5 mmol) and Na<sub>2</sub>CO<sub>3</sub> (15 mmol) in water (15 mL) were added to a solution of 2,2-dimethyl-propionyl chloride (5 mmol) in dichloromethane (15 mL) at ambient temperature and the reaction was stirred for 12 h. The organic layer was then separated, and the aqueous phase was extracted with additional dichloromethane (2 × 25 mL). The combined organic layers were dried over Na<sub>2</sub>SO<sub>4</sub> and reduced in vacuo. The residue was recrystallized from EtOAc/hexane to give (S)-3-(2',2'-dimethyl-propionyl)-amino-caprolactam (645 mg, 61%); δ<sub>H</sub> (500 MHz, CDCl<sub>3</sub>) 7.10 (1H, d, *J* 5.0, CHNH), 6.75 (1H, br s, CH<sub>2</sub>NH), 4.42 (1H, ddd, *J* 11, 5.5, 1.5, CHNH), 3.27–3.16 (2H, m, CH<sub>2</sub>NH), 2.03–1.89 (2H, m, 2 × ring CH), 1.83–1.71 (2H, m, 2 × ring CH), 1.45–1.28 (2H, m, 2 × ring CH) and 1.15 (9H, s, 3 × CH<sub>3</sub>).

**Biology.** Compounds were tested for their ability to inhibit chemokine-induced migration using the microtiter format trans-well migration assay, exactly as described previously.<sup>6a,7,10</sup> All migration assays were performed in Gey's balanced salt solution containing 1 mg/mL endotoxin-free BSA (in the absence of fetal calf serum), allowing migration to occur for 2 h at 37 °C. All compounds were solubilized in DMSO and added to both the top and bottom compartments of the trans-well migration plate at a constant final DMSO concentration of 1%.

The effect of the compounds on TNF-α upregulation in vivo was determined exactly as previously,<sup>7b,10</sup> except that the vehicle used was 0.6% DMSO 1% carboxymethylcellulose (final concentrations) in sterile water.

For pharmacokinetic analysis, male Sprague–Dawley rats (three animals per compound per route) were dosed with compound via the intravenous route (1 mg/mL) or the oral route by gavage (3 mg/mL). The vehicle for intravenous administration was 5% DMSO in 0.9% saline; the vehicle for oral administration was 1% carboxymethylcellulose in 0.9% saline. Animals received food and water ad libitum throughout. Blood was drawn at 5, 15, 30, 60, 120, 180, 240, and 480 min after dosing, and plasma was prepared. Drug concentration was determined by LC/MS/MS following extraction of 50 μL of plasma with 100 μL of 0.1% formic acid in acetonitrile, followed by centrifugation at 6000g for 5 min. An Atlantis column (20 mm × 2.1 mm; Waters) was used on a Sciex 4000 (Applied Biosystems) operating in TurboIonSpray positive mode, with a mobile phase gradient of 0.1% formic acid in aqueous buffer to acetonitrile over 3.5 min. An internal standard of related structure was used to correct for extraction efficiency. Pharmacokinetic parameters were estimated by standard noncompartmental methods, using Excel. Area under the curve (AUC) calculations used the linear trapezoidal rule

when plasma concentrations are rising and the log trapezoidal rule when concentrations are falling. Following intravenous dosing the concentration versus time curve was extrapolated from the first data point back to time zero by assuming an initial volume of 0.26 L/kg (plasma volume in a rat).

**Acknowledgment.** We thank Dr John Davies for crystallography and the EPSRC for financial assistance towards the purchase of the Nonius CCD diffractometer. D.J.G. is a director of, and D.J.F. is a consultant for, Funxional Therapeutics Ltd.

**Supporting Information Available:** Synthesis and characterization data for all compounds (CIF, PDF), in vitro and in vivo biological data. This material is available free of charge via the Internet at <http://pubs.acs.org>.

## References

- (1) (a) Gerard, C.; Rollins, B. J. Chemokines and disease. *Nat. Immunol.* **2001**, *2*, 108–115. (b) Horuk, R. Chemokine receptors. *Cytokine Growth Factor Rev.* **2001**, *12*, 313–335. (c) Rollins, B. J. Chemokines. *Blood* **1997**, *90*, 909–928. (d) Luster, A. D. Chemokines—Chemotactic cytokines that mediate inflammation. *N. Engl. J. Med.* **1998**, *338*, 436–445. (e) Thelen, M. Dancing to the tune of chemokines. *Nat. Immunol.* **2001**, *2*, 129–134.
- (2) Antonella Viola, A.; Luster, A. D. Chemokines and Their Receptors: Drug Targets in Immunity and Inflammation. *Annu. Rev. Pharmacol. Toxicol.* **2008**, *48*, 171–197.
- (3) (a) Ribeiro, S.; Horuk, R. The clinical potential of chemokine receptor antagonists. *Pharmacol. Ther.* **2005**, *107*, 44–58. (b) Carter, P. H. Chemokine receptor antagonism as an approach to anti-inflammatory therapy: 'just right' or plain wrong? *Curr. Opin. Chem. Biol.* **2002**, *6*, 510–525. (c) Allen, S. J.; Crown, S. E.; Handel, T. M. Chemokine: Receptor Structure, Interactions and Antagonism. *Annu. Rev. Immunol.* **2007**, *25*, 787–820.
- (4) (a) Vaidehi, N.; Schlyer, S.; Trabanino, R. J.; Floriano, W. B.; Abrol, R.; Sharma, S.; Kochanny, M.; Koovakat, S.; Dunning, L.; Liang, M.; Fox, J. M.; de Mendonca, F. L.; Pease, J. E.; Goddard, W. A., III.; Horuk, R. Predictions of CCR1 Chemokine Receptor Structure and BX 471 Antagonist Binding Followed by Experimental Validation. *J. Biol. Chem.* **2006**, *281*, 27613–27620. (b) Pasternak, A.; Goble, S. D.; Doss, G. A.; Tsou, N. N.; Butora, G.; Vicario, P. P.; Ayala, J. M.; Struthers, M.; DeMartino, J. A.; Mills, S. G. Yang, Conformational studies of 3-amino-1-alkyl-cyclopentane carboxamide CCR2 antagonists leading to new spirocyclic antagonists. *Bioorg. Med. Chem. Lett.* **2008**, *18*, 1374–1377. (c) L. Santella, J. B., III.; Gardner, D. S.; Yao, W.; Shi, C.; Reddy, P.; Tebben, A. J.; DeLucca, G. V.; Wacker, D. A.; Watson, P. S.; Welch, P. K.; Wadman, E. A.; Davies, P.; Solomon, K. A.; Graden, D. A.; Yeleswaram, S.; Mandekar, S.; Kariv, I.; Decicco, C. P.; Ko, S. S.; Carter, P. H.; Duncia, J. V. From rigid cyclic templates to conformationally stabilized acyclic scaffolds. Part I: The discovery of CCR3 antagonist development candidate BMS-639623 with picomolar inhibition potency against eosinophil chemotaxis. *Bioorg. Med. Chem. Lett.* **2008**, *18*, 576–585. (d) Thoma, G.; Beerli, C.; Bigaud, M.; Bruns, C.; Cooke, N. G.; Streiff, M. B.; Zerwes, H.-G. Reduced cardiac side-effect potential by introduction of polar groups: discovery of NIBR-1282, an orally bioavailable CCR5 antagonist which is active in vivo. *Bioorg. Med. Chem. Lett.* **2008**, *18*, 2000–2005.
- (5) (a) Vandercappellen, J.; Van Damme, J.; Struyf, S. The role of CXC chemokines and their receptors in cancer. *Cancer Lett.* **2008**, *267*, 226–244. (b) Biju, P.; Taveras, A.; Yu, Y.; Zheng, J.; Chao, J.; Rindgen, D.; Jakway, J.; Hipkin, R. W.; Fossetta, J.; Fan, X.; Fine, J.; Qiu, H.; Merritt, J. R.; Baldwin, J. J. Diamino-2,5-thiadiazole-1-oxides as potent CXCR2/CXCR1 antagonists. *Bioorg. Med. Chem. Lett.* **2008**, *18*, 228–231.
- (6) (a) Reckless, J.; Grainger, D. J. Identification of oligopeptide sequences which inhibit migration induced by wide range of chemokines. *Biochem. J.* **1999**, *340*, 803–811. (b) Reckless, J.; Tatalick, L. M.; Grainger, D. J. The pan-chemokine inhibitor NR58-3.14.3 abolishes tumour necrosis factor-α accumulation and leucocyte recruitment induced by lipopolysaccharide in vivo. *Immunology* **2001**, *103*, 244–254.
- (7) (a) Fox, D. J.; Reckless, J.; Warren, S. G.; Grainger, D. J. Design, synthesis, and preliminary pharmacological evaluation of *N*-acyl-3-aminoglutarimides as broad-spectrum chemokine inhibitors in vitro and anti-inflammatory agents in vivo. *J. Med. Chem.* **2002**, *45*, 360–370. (b) Fox, D. J.; Reckless, J.; Wilbert, S. M.; Greig, I.; Warren, S.; Grainger, D. J. Identification of 3-(Acylamino)azepan-2-ones as Stable

- Broad-Spectrum Chemokine Inhibitors Resistant to Metabolism in Vivo. *J. Med. Chem.* **2005**, *48*, 867–874.
- (8) (a) Grainger, D. J.; Reckless, J. Broad-spectrum chemokine inhibitors (BSCIs) and their anti-inflammatory effects in vivo. *Biochem. Pharmacol.* **2003**, *65*, 1027–1034. (b) Naidu, B. V.; Farivar, A. S.; Krishnadasan, B.; Woolley, S. M.; Grainger, D. J.; Verrier, E. D.; Mulligan, M. S. Broad-spectrum chemokine inhibition ameliorates experimental obliterative bronchiolitis. *Ann. Thorac. Surg.* **2003**, *75*, 1118–1122. (c) Wilbert, S. M.; Engrissei, G.; Yau, E. K.; Grainger, D. J.; Tatalick, L.; Axworthy, D. B. Quantitative Analysis of a Synthetic Peptide, NR58–3.14.3, in Serum by LC-MS with Inclusion of a Diastereomer as Internal Standard. *Anal. Biochem.* **2000**, *278*, 14–21.
- (9) Schroff, R. W.; Touvay, C.; Culler, M. D.; Dong, J. Z.; Taylor, J. E.; Thurieau, C.; McKilligin, E. The Toxicology of Chemokine Inhibition. *Mini-Rev. Med. Chem.* **2005**, *5*, 849–855.
- (10) Frow, E. K.; Reckless, J.; Grainger, D. J. Tools for anti-inflammatory drug design: in vitro models of leukocyte migration. *Med. Res. Rev.* **2004**, *24*, 276–298.

JM900133W